

KRITTIKA SUMMER PROJECTS 2023

Exploring the Radio Sky

Mehul Goyal

KRITTIKA SUMMER PROJECTS 2023

Exploring the Radio Sky

Mehul Goyal¹

¹IIT Bombay

Copyright © 2023 Krittika IITB
PUBLISHED BY KRITTIKA: THE ASTRONOMY CLUB OF IIT BOMBAY
GITHUB.COM/KRITTIKAIITB
Project Code Repository: KSP-Exploring The Radio Sky
First Release, September 2023

Abstract

In this project, we explore Radio Astronomy, from the basics to Fast Radio Bursts. We start with an introduction to Radio Astronomy, exploring its history and learning the basics. Radio Sky unravels the otherwise hidden universe to other Electromagnetic Spectrum regions. We deeply dive into understanding Radiation Physics which is crucial for Astronomy, exploring Blackbody Radiation, Rayleigh-Jeans Approximation, Interference and Polarization. In this project, we also build on our understanding of the design, structure and functioning of Radio Telescopes, Aperture Synthesis and Deconvolution of Captured Images. Applications of learnt theory involve activities on the Gravitational Wave detection GW170817 produced by the merger of two neutron stars, which was the first to be confirmed by non-gravitational means. We plot the light curve of GW170817 and use the method of Markov Chain Monte Carlo to find the most-likely model for the light curve. We use the Smooth Broken Power Law to model the light curve. In the project, we also gained experience in the process of deconvolution of images using CASA and used the imstat library to analyse the cleaned image as well. In the final part, we explore Fast Radio Bursts. Our activity aimed to calculate the value of the Dispersion Measure for the detected signal from a pulsar.

Contents

I

Part One

1	Introduction to Radio Astronomy	7
1.1	A Brief History	7
1.2	Fundamentals of Radio Waves	8
1.2.1	Electromagnetic Radiation	8
1.2.2	Spectroscopy	8
1.2.3	Sky Coordinate System : Declination and Right Ascension	9
1.3	Radio Maps	10
1.4	Activities	11
1.4.1	Activity 1	11
1.5	Activity 2	12
2	Introduction to Radiation Physics	13
2.1	Definitions	13
2.2	Blackbody Radiation	14
2.3	Rayleigh-Jeans Approximation	17
2.4	Brightness Temperature	17
2.5	Interference of Light	18
2.6	Polarization and Stokes Parameters	18
2.6.1	Stokes Parameters	18
2.7	Activities	19
2.7.1	Plotting Galaxy Rotation Curve	19

3	Radio Telescopes	21
3.1	Primary Reflectors	22
3.2	Beam Pattern	24
3.3	Feeds	24
3.4	Surface Errors	25
3.5	Noise, Noise Temperature and Antenna Temperature	25
4	Aperture Synthesis (Interferometry)	27
4.1	Why Aperture Synthesis ?	28
4.2	Two Element Interferometer	29
4.2.1	Response of Multiplicative Interferometer	30
4.3	Fringe Pattern	30
4.3.1	Calibration	31
4.4	Visibility	31
4.5	Synthesising Image	32
4.5.1	Casa Activity	33

II

Part Two

5	GW170817 - Binary Neutron Star Merger	37
5.1	Introduction	37
5.2	What are Light Curves ?	37
5.3	Markov Chain Monte Carlo	38
5.4	Smooth Broken Power Law	39
5.5	Data Analysis	40
6	Fast Radio Bursts	43
6.1	What are Transients ?	43
6.2	Dispersion Measure	44
6.3	Activity - Finding DM of a Burst	45
	Bibliography	47
	Books	47

Part One

1	Introduction to Radio Astronomy	7
1.1	A Brief History	
1.2	Fundamentals of Radio Waves	
1.3	Radio Maps	
1.4	Activities	
1.5	Activity 2	
2	Introduction to Radiation Physics	13
2.1	Definitions	
2.2	Blackbody Radiation	
2.3	Rayleigh-Jeans Approximation	
2.4	Brightness Temperature	
2.5	Interference of Light	
2.6	Polarization and Stokes Parameters	
2.7	Activities	
3	Radio Telescopes	21
3.1	Primary Reflectors	
3.2	Beam Pattern	
3.3	Feeds	
3.4	Surface Errors	
3.5	Noise, Noise Temperature and Antenna Temperature	
4	Aperture Synthesis (Interferometry)	27
4.1	Why Aperture Synthesis ?	
4.2	Two Element Interferometer	
4.3	Fringe Pattern	
4.4	Visibility	
4.5	Synthesising Image	



1. Introduction to Radio Astronomy

1.1 A Brief History

Radio Astronomy had its beginnings in December of 1932 when Karl Jansky, an employee at Bell Labs, achieved the first successful detection of astronomical radio emissions originating from the center of our galaxy, the Milky Way. Intrigued by Jansky's groundbreaking discovery, Grote Reber constructed a 30-foot antenna and successfully mapped radio emissions from the galaxy at a higher resolution than Jansky's. Notably, Reber identified additional peaks in signal strength beyond the strong emission from the Milky Way's center: one in the constellation Cassiopeia, now known as Cas A, which is a super nova remnant, and another in Cygnus, referred to as Cyg A, a radio galaxy. These significant findings were published in astronomical journals in 1940 and 1944, marking the first-ever radio wavelength observations to be published as such.

During World War II, radar technology saw significant advancements for military purposes. After the war, J.S. Hey, along with S. J. Parson, J. W. Phillips, and G. S. Stewart, continued with radar and radio studies, leading to several discoveries. In 1945, Hey and his colleagues made the discovery that meteors create ionization trails that reflect radio waves. In 1946, they conducted a more detailed radio sky mapping compared to Reber's work and identified the variable radio emission from Cygnus. They also recognized Cyg A as a distinct source separate from the extended radio emission associated with the Milky Way. In 1948, their work established the association of solar radio bursts with sunspots and solar flares.

The idea of utilizing radio observations as a major avenue for studying vast regions of the universe was proposed in 1944 by the renowned Dutch astrophysicist Jan Oort, who suggested to Hendrik van de Hulst to calculate the wavelength of the hydrogen emission line caused by the electron's spin flip. Van de Hulst's calculations predicted that this transition would emit radiation at a 21 cm wavelength. The first detection of the 21-cm line occurred in 1951 when Harold Ewen and Edward Purcell, researchers at Harvard, successfully observed it. This 21-cm line remains a

valuable tool for mapping the distribution of hydrogen atoms throughout space. In 1946, as a crucial step towards high-resolution radio astronomy observing techniques, Sir Martin Ryle and D. D. Vonberg conducted the first astronomical observation using a pair of radio antennas as an interferometer. Subsequent interferometric observations by various investigators allowed precise measurements of the positions of bright radio sources. Throughout the 1960s, radio astronomy yielded groundbreaking discoveries of quasars and pulsars, as well as the cosmic microwave background, with the latter two discoveries earning Nobel Prizes.

1.2 Fundamentals of Radio Waves

1.2.1 Electromagnetic Radiation

Radio Waves are Electromagnetic Waves and are produced when a charged particle undergoes acceleration. They are essentially orthogonally oscillation electric and magnetic fields. The velocity , frequency and wavelength of a wave are related by the equation

$$\lambda = h\nu$$

We can also describe EM Waves by a particle known as photon. A photon has no mass and its energy is given by

$$E = h\nu$$

, where h is the Plank's Constant = 6.626×10^{-34} J s.

The radio band encompasses a wide spectrum of frequencies capable of traversing Earth's atmosphere without hindrance, making it an ideal realm for detecting and studying electromagnetic radiation from space. This region, often referred to as the "radio window," spans from 10 MHz (1×10^7 Hz) to 300 GHz (3×10^{11} Hz), corresponding to wavelengths between 30 m and 1 mm. Radio photons within this range carry energies ranging from approximately 10^{-19} to 10^{-15} ergs, which are incredibly minute. The boundaries of this radio window are determined by atmospheric and ionospheric phenomena.

At lower frequencies, particularly below 10 MHz, the ionosphere contains free electrons that readily absorb and/or reflect radiation, limiting observations at these wavelengths. On the higher-frequency end, absorption by atmospheric constituents such as H₂O and O₂ obstructs the passage of radiation from space. To overcome this, radio observatories operating at millimeter wavelengths are highly desirable and should ideally be situated at elevated, arid locations to minimize interference caused by water vapor.

1.2.2 Spectroscopy

A powerful tool for analyzing the detected radiation is to examine its spectrum (a plot or display of the amount of radiation vs. frequency or wavelength), as the details of a source's spectrum contain much valuable information about the physics of the source. The three basic types of spectra are as follows :

Continuous Spectra : When a radiation source emits at all frequencies over a range, the spectrum is called a continuous spectrum and the emitting object is called a continuum source. A classic example of a continuum source is an

incandescent lamp.

Emission Spectra : When a radiating object emits radiation only at some very specific frequencies, the spectrum contains a set of discrete bright lines. These lines of light are called emission lines. Different atoms and molecules emit different sets of frequencies, and so the composition of a radiation source can be identified by determining the frequencies of the emission lines. This is one example of how spectroscopy is such a powerful tool in Astronomy

Absorption Spectra:When radiation from a continuous source passes through a cool, transparent gas composed of atoms or molecules, some of these atoms or molecules can absorb photons from the radiation, causing them to transition to higher energy levels allowed by their structure. For an observer located beyond the cool gas, the resulting spectrum will display the continuous spectrum of the background source, but with specific frequencies darkened or attenuated. When plotting the intensity of the radiation against its frequency, these darkened frequencies appear as dips or regions of decreased intensity, commonly referred to as absorption lines.

It's worth noting that the frequencies at which the atoms or molecules absorb the radiation are identical to the frequencies at which they can emit radiation. As a result, the chemical composition of a gas cloud can be determined by examining the frequencies of the absorption lines it produces. This property allows scientists to identify the elements or molecules present in distant celestial objects by analyzing the absorption lines present in their spectra.

1.2.3 Sky Coordinate System : Declination and Right Ascension

To effectively locate and observe objects in the sky, a consistent coordinate system is essential. The celestial sphere serves as a model, resembling a globe of the surrounding sky with the Earth at its center. Within this system, two key coordinates, declination and right ascension, function similarly to latitude and longitude but pertain to positions of celestial objects, such as stars, on the celestial sphere. Together, they form the equatorial coordinate system, also known as the celestial coordinate system, used for identifying the location of a celestial object relative to the Earth's equator. This system is based on projecting the Earth's equator infinitely into space.

Declination corresponds to the astronomical equivalent of latitude and measures the angular distance of a point north or south of the Celestial Equator, which is an extension of the Earth's equator into space. The declination ranges from -90° (South Celestial Pole) to +90° (North Celestial Pole).

On the other hand, right ascension is analogous to longitude and represents the angular distance of an object measured eastward from the Vernal Equinox. Unlike longitude, right ascension is usually measured in hours, minutes, and seconds, with 24 hours making a full circle (360°). This means that each hour corresponds to 15 degrees (1 hour = 15°).

Both right ascension and declination remain constant over time and are not centered on the observer. However, for practical observational purposes, a system that describes the way a specific observer (or telescope) views the sky at any given moment is necessary. Hence, an observer-centered coordinate system is used, which is the Alt-Az system.

Altitude is the measurement of the angular height of an object above the observer's horizon at a particular time. An object at the horizon has an altitude of 0° , while an object directly overhead at the zenith has an altitude of 90° .

Azimuth is the angular position perpendicular to the altitude and refers to the object's position along the horizon relative to due north. When an object is north of the zenith, its azimuth is 0° , and if it is south of the zenith, its azimuth is 180° . Azimuths of $+90^\circ$ and 270° correspond to due east and due west, respectively. These altitude and azimuth coordinates allow observers to precisely describe the position of celestial objects as seen from their specific location on Earth at any given moment.

1.3 Radio Maps

When presenting the structure of a source at radio wavelengths or other wavelengths, the presenter has several choices for how to best display the two-dimensional data. One common method is using a contour map, where lines of constant intensity, known as contours, are plotted. A region with a large number of closely spaced contours indicates rapid changes in intensity with position.

Another approach is using a gray scale map, where variations in brightness are directly represented by shades of gray. In this type of map, black represents the most intense areas, while white corresponds to the least intense regions. This method offers a slightly more intuitive representation of the source's structure.

False Color Maps can also be employed, where the color does not represent different wavelengths but rather different levels of brightness. These maps often include a color-wedge alongside them to indicate the relationship between color and brightness. False Color Maps not only create visually appealing images but can also aid in the analysis of the data.

1.4 Activities

1.4.1 Activity 1

In this activity we imaged a source at different wavelengths, in radio, infrared and visible spectrum. This is an example of how a source can be completely invisible in one part of EM spectrum, while you can image it in its full glory in some other part of the spectrum. In this particular example, in Radio frequencies we observe the beautiful jets from the source(Figure 1.2), whereas in visible we do not see anything(Figure 1.1).

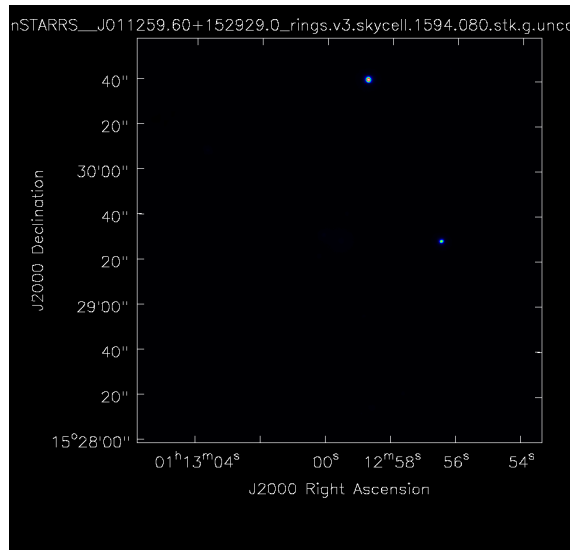


Figure 1.1: Source in Visible Wavelengths

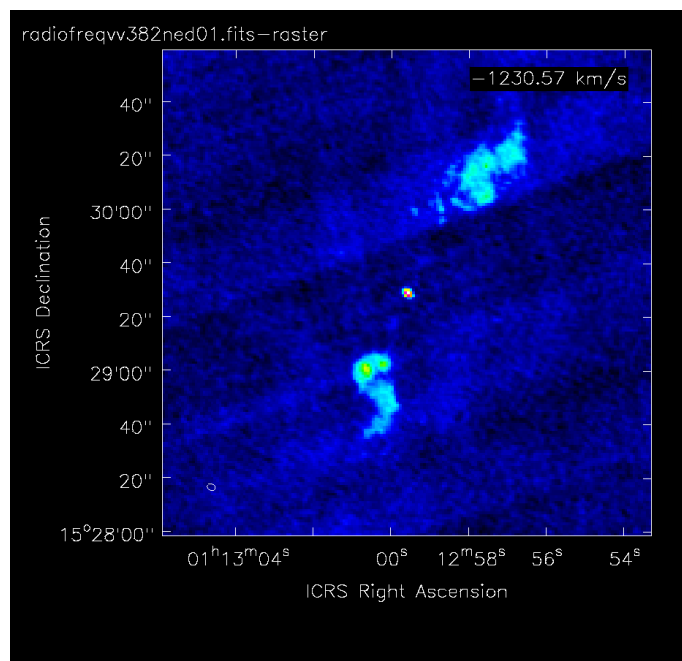


Figure 1.2: Source in Radio Wavelengths

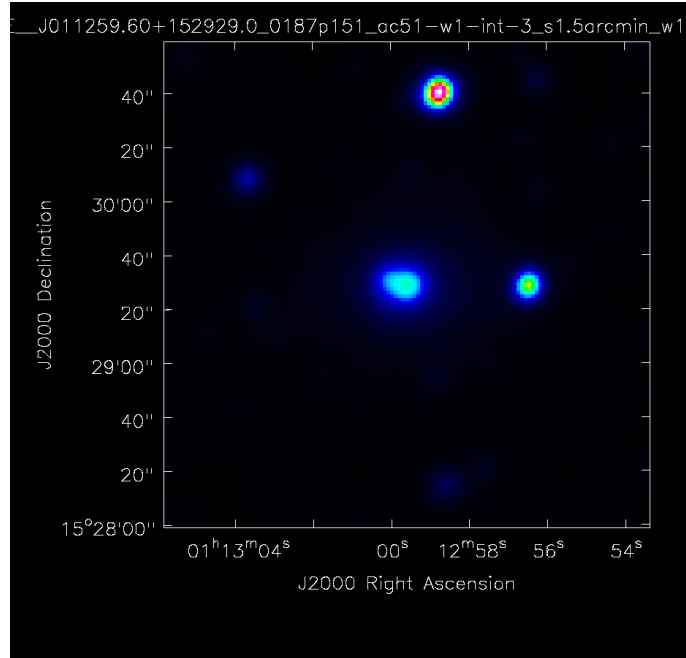


Figure 1.3: Source in Infrared Wavelengths

1.5 Activity 2

We also plotted lightcurve of GW170817 (named by discovery date - 17 August 2017) which was the first ever detection in electromagnetic waves of a compact binary merger event of two neutron stars following its detection in gravitational waves with LIGO (Figure 1.4). The Flux Densities in micro-Jansky have been plotted on the Y-axis against Day of Observation on X-axis.

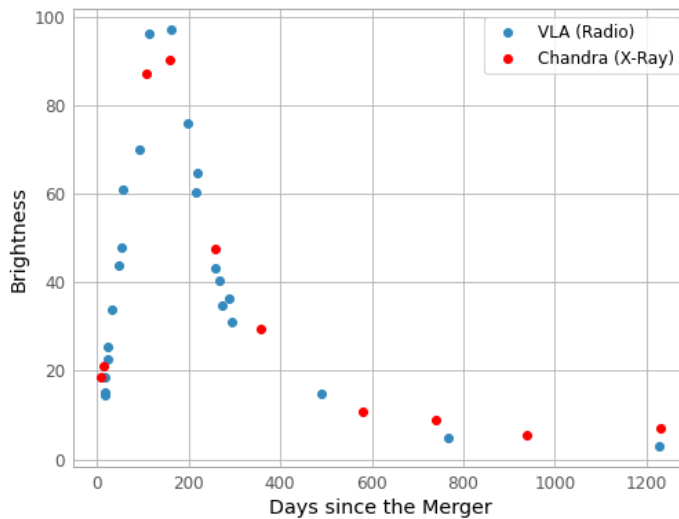
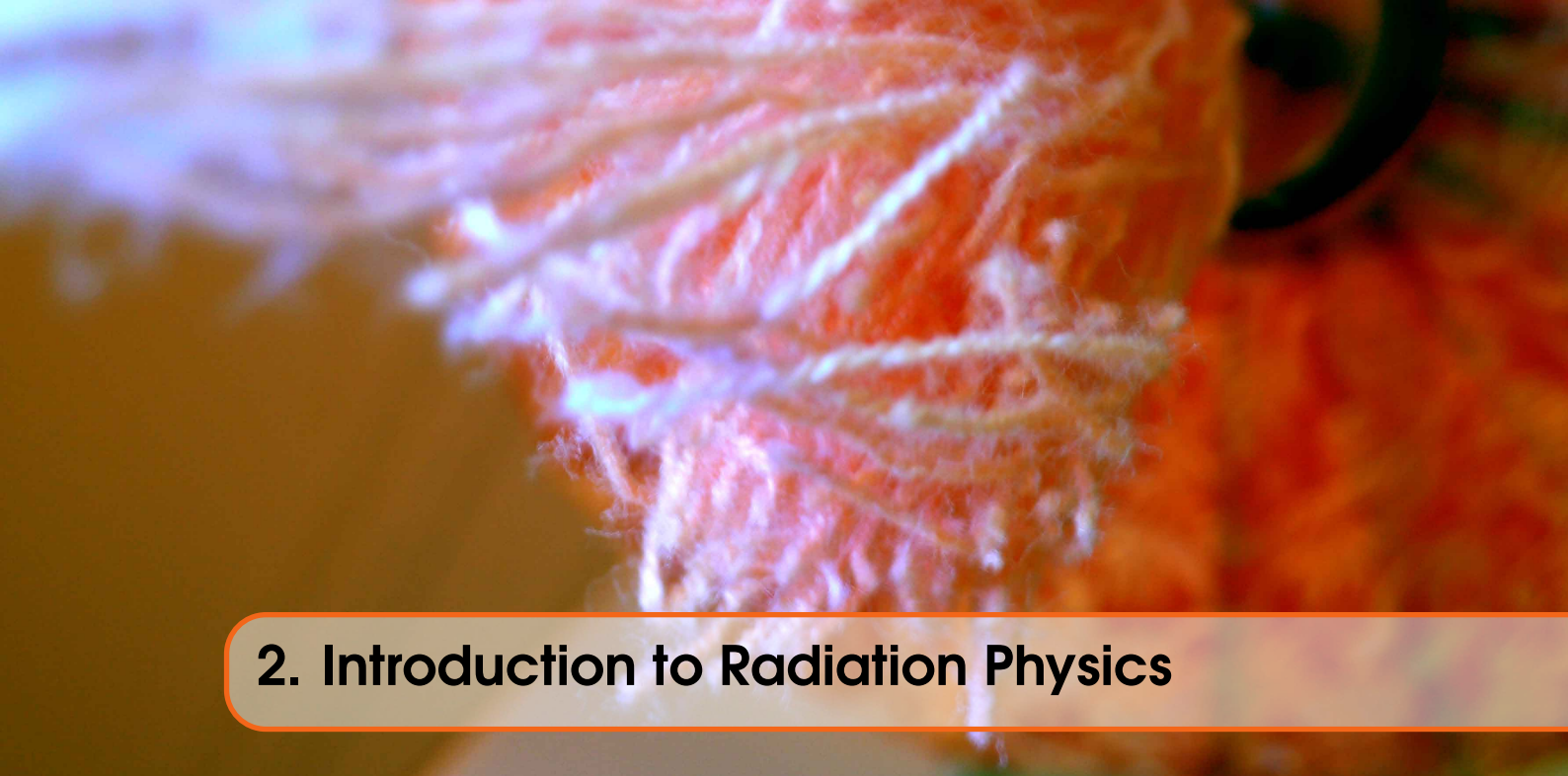


Figure 1.4: Light Curve of GW170817.



2. Introduction to Radiation Physics

2.1 Definitions

LUMINOSITY : Luminosity (L) or power is the rate at which energy is emitted. Its SI units are $J s^{-1}$ or watts ($1 W = 1 J s^{-1}$) and $ergs^{-1}$ in cgs. One calculates a source's luminosity or power by dividing the amount of energy emitted by the length of time over which the energy was emitted. This yields the rate of emission.

FLUX : The amount of light energy per unit time per unit area. The units of flux are $J s^{-1} m^{-2}$ or $W m^{-2}$ (SI) and $ergs s^{-1} cm^{-2}$ in (cgs). The Flux received by our Telescope is given by the equation :

$$P = L \frac{A_{eff}}{4\pi d^2}$$

FLUX DENSITY : Flux density (F_ν or F_λ) is the flux per unit frequency in the observed spectral range, and it equals the detected flux divided by the width in frequency of the observation. Therefore,

$$F_\nu = \frac{F}{\Delta\nu}$$

where:

$\Delta\nu$ is the bandwidth, or the range in frequency of the detected EM waves. The symbol S_ν (rather than F_ν) is often used by radio astronomers to represent flux density per unit bandwidth. When working at visible wavelengths, astronomers tend to measure flux density in terms of wavelength rather than frequency, so flux density is also often defined as flux per unit wavelength.

$$F_\lambda = \frac{F}{\Delta\lambda}$$

Although these two quantities are the same conceptually, they are not the same quantitatively (Their dimensions are different). The Flux Density is the characteristic of the source that we want to infer from the data. The amount of power a telescope collects from a source of given flux density is given by

$$P = F_\nu A_{eff} \Delta\nu$$

We get very small numbers for Flux Density measurements in SI or CGS Units. Ergo, Radio Astronomers have defined a unit of Flux Density named after Father of Radio Astronomy Karl Jansky. In terms of SI Units, 1 Jansky is defined as :

$$1 \text{ Jansky} = 10^{-26} \text{ W m}^{-2} \text{ Hz}^{-1}$$

INTENSITY : Intensity is the Flux Density per unit solid angle. It is also a direct measure of surface brightness of the source. If you know the solid angle of the source (Ω), you can calculate the source's average intensity by dividing the source's Flux density with the solid angle. The units of Flux Density can be given by $\text{W m}^{-2} \text{ Hz}^{-1} \text{ sr}^{-1}$. Again I_ν and I_λ , though conceptually same are quantitatively very different. The expression for I_ν :

$$I_\nu = \frac{L}{4\pi d^2 \Delta\nu \Omega}$$

One of the most important aspects of Intensity is that it is independent of the distance from the source and is a direct measurement of the Surface Brightness of the Source.

2.2 Blackbody Radiation

Max Planck's discovery that the spectrum of the radiation emitted by hot, opaque objects can be fit by a model that assumes quantized units of energy led him to win a Nobel Prize in 1918. A body which absorbs all radiation incident on it, reflects none and prevents transmission of light is called a *blackbody*, and is called opaque. The radiation emitted by such a body is called blackbody radiation. Thus, Blackbody Radiation is maximum amount of radiation that an ordinary body of a particular temperature will emit solely as an attempt to cool. The resultant radiation emitted from a body can be modelled as a cloud of photons at the same temperature as the body itself. When the photons have been thermalized, statistics can describe the distribution of energies of the photons, that is, the relative number of photons carrying each small range of energy. In other words, with blackbody radiation, the photons have achieved a thermal distribution of energies. The energy distribution function of photons, (Number of photons as a function of their energy) is directly related to spectral distribution, i.e. Intensity v/s Frequency. The frequency is proportional to the energy (since for photons $E = h\nu$) and the intensity at a given frequency is proportional to the flux of photons at that frequency.

The *Plank's Function* provides a mathematical description of the spectrum of the light emitted by blackbodies. In terms of the emitted flux per unit frequency interval per unit steradian, the Planck function is given by:

$$B_\nu = \frac{2h\nu^3}{c^2} \frac{1}{e^{\frac{h\nu}{kT}} - 1}$$

Where,
 h is the Plank's Constant,
 k is the Boltzmann Constant,
 c is the Speed of Light,
 ν is the frequency of observation, and
 T is the temperature of radiating body in Kelvins

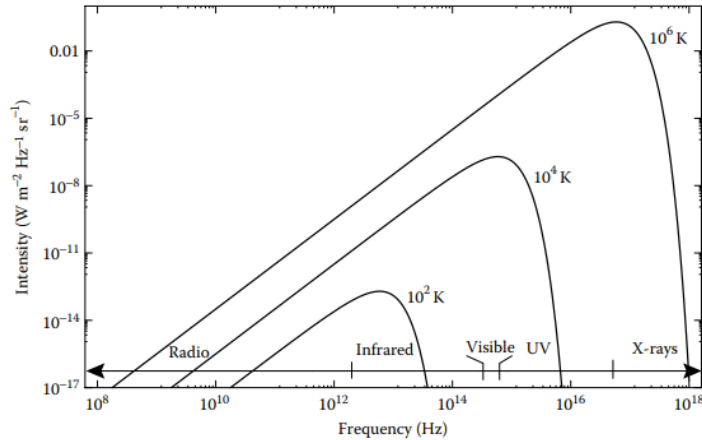


Figure 2.1: Log-log plot of $B_\nu(T)$ versus ν for three different temperatures.
Source : Fundamentals of Radio Astronomy : Observational Methods

Plank's Function can also be expressed as Flux per unit *wavelength* per steradian, which is B_λ , and is given by :

$$B_\lambda = \frac{2hc^2}{\lambda^5} \frac{1}{e^{\frac{hc}{\lambda kT}} - 1}$$

Again, B_λ and B_ν being conceptually the same, are not the same quantities. They are not even the same function. The total flux of radiation (W m^2) emitted by the body can be obtained by integration of the Planck function over frequency and solid angle. The result shows that the total flux is proportional to the fourth power of the body's temperature and is called *Stefan-Boltzmann Law* :

$$F = \sigma T^4$$

where, σ is known as the *Stefan-Boltzmann Constant* = 5.67×10^{-8} . A key feature of Blackbody Radiation, as apparent in figures 2.1 and 2.2 is that value of B_ν increases with temperature of every frequency, which means that as the temperature of blackbody increases, it emits more energy at every frequency. In practical terms, this has an important implication that at any given frequency, any particular value of intensity corresponds to exactly one temperature. Note that the blackbody curves for different temperatures never cross. Therefore, even if you know the intensity of an opaque object at only a single frequency, and if the radiating

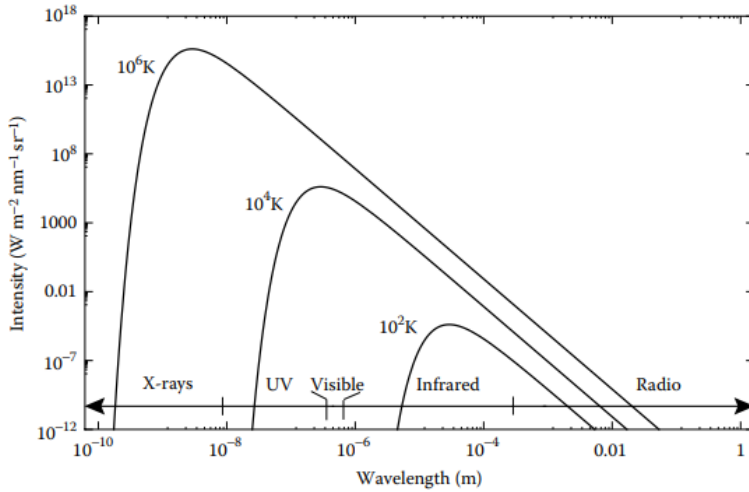


Figure 2.2: Log-log plot of $B_\lambda(T)$ versus λ for three different temperatures.
Source : Fundamentals of Radio Astronomy - Observational Methods

source is a blackbody, then you can infer the temperature of the source by this single intensity measurement. The Intensity can be inferred from measurements of both flux density and angular size of the source. The universe's cosmic microwave background (CMB), which fills the entire sky, is a great example of a situation where temperature can be inferred from a single-frequency observation. We performed the activity to calculate the temperature corresponding to Cosmic Microwave Background. We fitted the Plank's Function to a given dataset and got the value of temperature to be 2.7 Kelvins (Figure 2.3). An important equation to remember, which we do not go into derivation of, is that average Kinetic Energy of Photons at a given temperature of Photon Gas is given by the equation $\langle E \rangle = 2.7kT$, where k is the Boltzmann's Constant.

Figures 2.1 and 2.2 show that peaks of the Plank Spectrum depends only the temperature of the body. As the temperature increases, the peak of the Blackbody spectrum occurs at a higher frequency. The peak can be obtained by differentiating B_ν and B_λ with respect to temperature and equating them to be zero. This gives us Wien's Displacement Law. For B_ν ,

$$\nu_{peak} = (5.879 \times 10^{-10})T$$

For B_λ ,

$$\lambda_{peak} = (2.898 \times 10^{-3})T$$

An important thing to note here is that the above two equations do not give the same information, which is inherent due to the fact that I_ν and I_λ are two different functions. You can check this by substituting $c = \nu\lambda$ in Planks Funnction for frequency, you will not get the correct expression for B_λ . The correct conversion

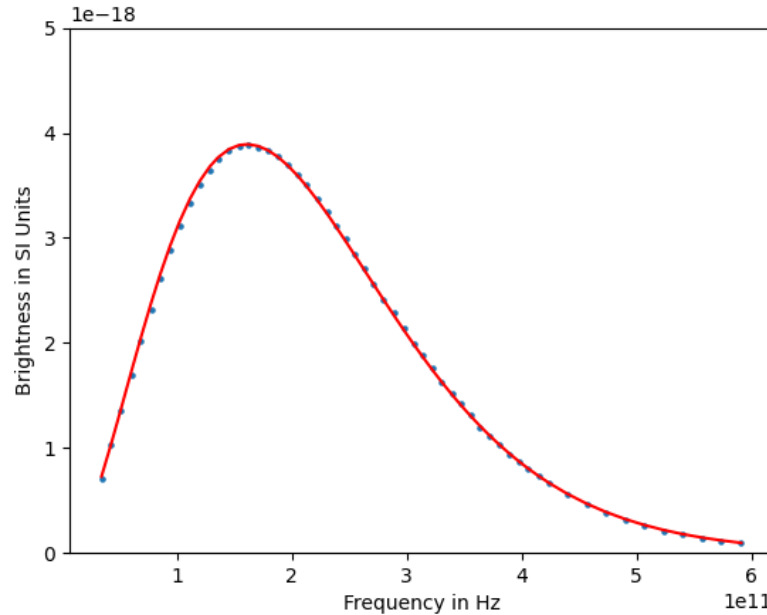


Figure 2.3: Fit of Planks Function to Cosmic Microwave Background.
Source : Fundamentals of Radio Astronomy : Observational Methods

factor for converting between I_ν and I_λ is given by :

$$I_\lambda = \frac{c}{\lambda^2} I_\nu$$

If you use this conversion in either of the Planck functions, you will find that one does convert to the other.

2.3 Rayleigh-Jeans Approximation

At most radio wavelengths, Plank's Function can be approximated by a much simpler expression. At most radio wavelengths, the frequency ν is so small that, $\frac{h\nu}{kT} \ll 1$ for any reasonable temperature. The exponent in denominator of Plank's Function can be expanded and approximated using Taylor series to yield:

$$B_\nu = \frac{2kT}{\lambda^2}$$

2.4 Brightness Temperature

Brightness Temperature (T_B) is defined as :

$$B_\nu(T_B) = \frac{2h\nu^3}{c^2} \frac{1}{e^{\frac{h\nu}{kT_B}} - 1}$$

Brightness Temperature is a property of the *radiation* not *source*. Brightness Temperature is a measure of the intensity and is equal to the temperature the source would

have if it were a perfect blackbody. At low frequencies, where the Rayleigh-Jeans approximation applies, the brightness temperature is directly proportional to intensity.

$$T_B = \frac{\lambda^2}{2k} I_\nu$$

2.5 Interference of Light

Coherent Radiation : The radiation is said to be *coherent* if the Electromagnetic waves comprising the incoming radiation have the same frequency and exactly the same phase. In reality no light is perfectly coherent. The incoming radiation always has a range of frequencies with different phases and travel directions. These two aspects of radiation are called as *temporal coherence* and *spatial coherence* respectively. A range of frequencies reduces the temporal coherence and a range of travel directions degrades the spatial coherence. When we are first introduced to interference patterns and Young's Double Slit Experiment, we are taught by assuming a perfectly coherent beam of light incident on the double slit. But it's important to realise that for interference pattern to appear, light only needs to partially coherent, as is evident by the original experiment of Young, in which he used sunlight. He used a pinhole to introduce spacial coherence in sunlight, and the fact that human eyes can detect only a range of wavelengths introduced the the temporal coherence, and with the ability of human eyes to distinguish different colours, Young was able to observe an interference pattern. The concept that light does not have to be 100 percent coherent, but only partially coherent,to produce an interference pattern is very important to appreciate when learning about radio telescopes and doing radio astronomy observations, and for understanding technique of interferometry which is used to increase resolution of radio telescopes.

2.6 Polarization and Stokes Parameters

We know light is essentially orthogonally oscillating electric and magnetic fields. Polarization of incoming light is an essential parameter to understand physics of the source. *Plane polarized* light is the one in which the electric field oscillates only in one plane (the magnetic field is always perpendicular to electric field at all instants of time), whereas *circular polarized* light is the one in which the electric field vector rotates and has constant amplitude , tracing out a circle. The direction of net electric field at any instant of time can be modelled by two orthogonal oscillating electric field, who net vector sum at any instant gives the direction of electric field at that instant. We can invoke the concept of *Lissajous Figures* and understand when the light will be plane or circularly polarized. When both orthogonal electric field oscillate in-phase, we have a plane polarized light, and when there is 90° phase difference between them, we get circularly polarized, and elliptical polarized light beam for other values of phase difference.

2.6.1 Stokes Parameters

Sir George Stokes developed a set of four parameters as a means of quantifying polarization.

The first parameter I is total intensity of all radiation, and is basically sum of intensities of two orthogonal polarizations. We can choose two orthogonal bases polarizations for the purpose, which can be the two opposite circular polarizations(left and right) or two orthogonal linear polarizations.

$$I = I_x + I_y$$

$$I = I_R + I_L$$

The second parameter Q is difference in intensities of two linear polarizations.

$$Q = I_x - I_y$$

The third parameter U is very similar to the second, but involves a rotation of the x- and y-axes by 45° . If we call these shifted axes a and b, so that I_a is the intensity of light that is linearly polarized along an axis halfway between the x- and y-axes and I_b in the intensity of light polarized 90° relative to a, then

$$U = I_a - I_b$$

The fourth parameter, V , is equal to the difference in the intensities of the left and right circular polarizations, so

$$U = I_R - I_L$$

Q and U determine the amount of net linear polarization (L), where L is

$$L = \sqrt{Q^2 + U^2}$$

In unpolarized light, Q, V and U are all zero.

With elliptical polarization, the angle of major axis of the ellipse, relative to x and y , as chosen above as bases, is given by

$$\theta = \frac{1}{2} \tan^{-1} \left(\frac{U}{Q} \right)$$

The advantage of using Stokes Parameters for describing polarization is that they are all measures of Intensity.

2.7 Activities

2.7.1 Plotting Galaxy Rotation Curve

The Hydrogen 21 cm line is a very important spectral line in astronomy. Whenever a hydrogen atom forms, the electron within it will spontaneously de-excites until it's in the lowest (1s) state of the atom. With a 50/50 chance of having those spins of the electron and proton aligned, half of those atoms will be able to quantum tunnel into the anti-aligned state, emitting radiation of 21 centimeters (1420 MHz) in the process. In this activity, we used synthetic spectra of galaxies at different distances and we fit for doppler velocity of 21cm line for each distance. To do so, we fit a gaussian to spectral line and determined the central frequency and use the displacement from expected value to find the velocity. Then we plot the velocities as a function of distance from the centre of our galaxy to get the *Galaxy Rotation Curve*.

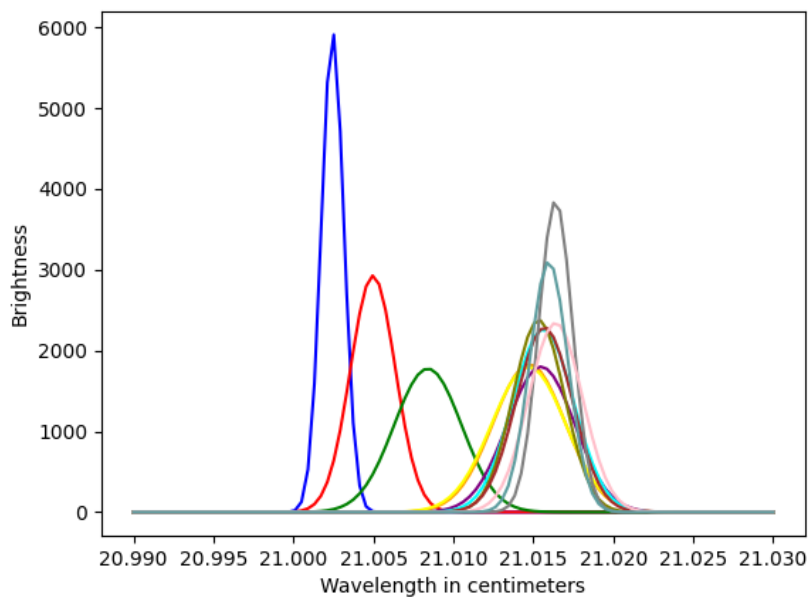


Figure 2.4: Best fit Gaussians to Spectral data from Galaxies

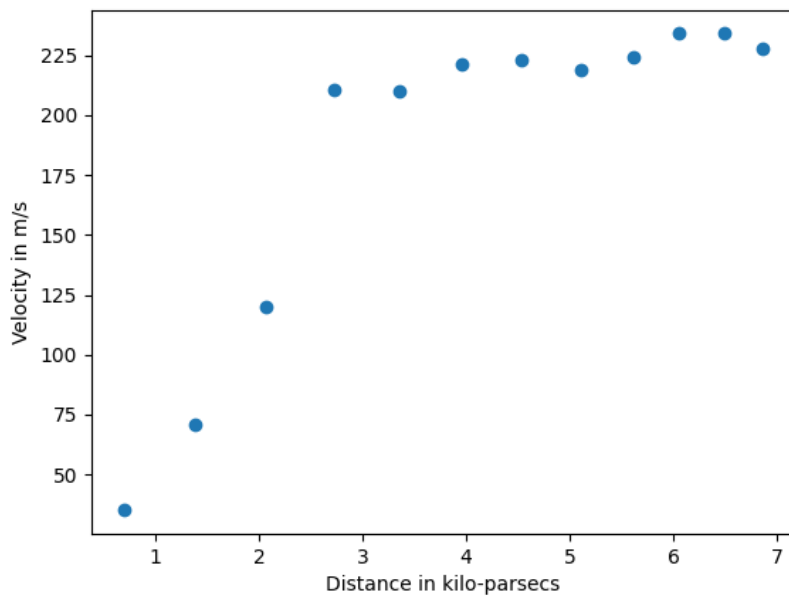


Figure 2.5: Galaxy Rotation Curve

3. Radio Telescopes

Observing with a radio telescope can be very different from using a visible-wavelength telescope. The Sun does not light up the whole sky at radio wavelengths, as it does at visible wavelengths. The blue daytime sky you see is sunlight that is scattered by the atmosphere, which scatters blue light to a greater extent than the longer visible wavelengths. At radio wavelengths, there is no scattering by the atmosphere at all. Therefore, the daytime sky is dark at radio wavelengths, and so radio observations can be made during day or night. At long radio wavelengths, observations can occur even with a cloud-covered sky since clouds are transparent at these frequencies. At shorter radio wavelengths, though, the water in clouds is a significant source of light loss, and so shorter-wavelength observations require clear weather. Radio telescopes operating at these short-radio wavelengths are often placed in high and dry sites to minimize this loss.

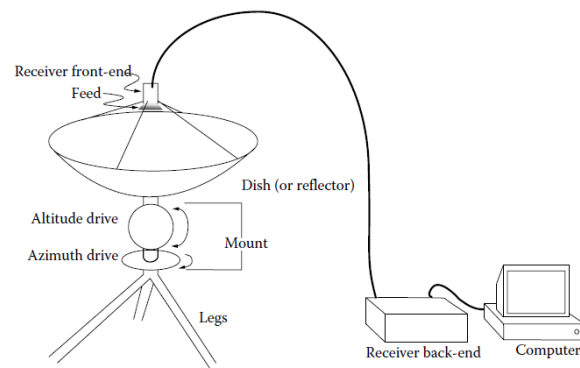


Figure 3.1: A Traditional Primary Reflector Radio Telescope.
Source : Fundamentals in Radio Astronomy : Observational Methods

The component of the telescope responsible for collecting signals is called *antenna*

or reflectors. By definition, an antenna is a device that couples electromagnetic wave in free space to confined electromagnetic waves in transmission lines of the telescope. The transmission lines carry the electromagnetic signal to the receiver. The reflectors are generally parabolic in shape to focus the collected parallel radiation to a particular point, the *focus* of the telescope. At long radio wavelengths, simple *dipole antennas* can be used as the first element. The famous Murchison Widefield Array (MWA) is one such example of a radio telescope, where first element is a dipole antenna. Two other words that are commonly used, and which



Figure 3.2: Murchison Widefield Array

help to avoid the misuse of the word antenna, are the dish, which is often used to refer to the reflector, and the feed, which is the device that couples the radiation concentrated by the reflector into a transmission line.

3.1 Primary Reflectors

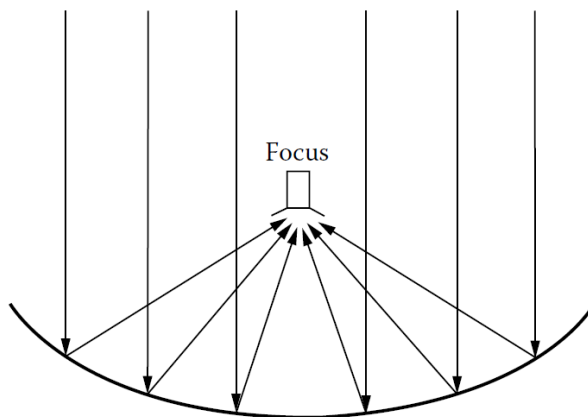


Figure 3.3: Primary Parabolic Reflector. Source : Fundamentals in Radio Astronomy : Observational Methods

The dishes of telescopes are generally parabolic in shape. The waves coming

from a an astronomical source can be approximated as parallel rays due to large magnitude of the distances involved. Figure 3.3 depicts the reflection of the parallel waves from the astronomical source and their arrival at the focus of the reflector. If the direction of the source in the sky is not perfectly inline with the axis of the telescope, then the parallel waves are not focused at the primary focus of the reflector, but at some other point. Therefore, parabolic surfaces have a defined focal plane.

Figure 3.3 shows a feed located at the focus of the telescope. We can use multiple feeds also. Most radio telescopes (and visible-light telescopes as well) are of *Cassegrain* design, instead of the primary-focus configuration. In a *Cassegrain* telescope, a second reflector (or mirror) is placed before the focal plane of the primary reflector to redirect the waves to another focal point (*the secondary focus*) at or behind the vertex of the primary reflector. This arrangement is shown in Figure 3.4.

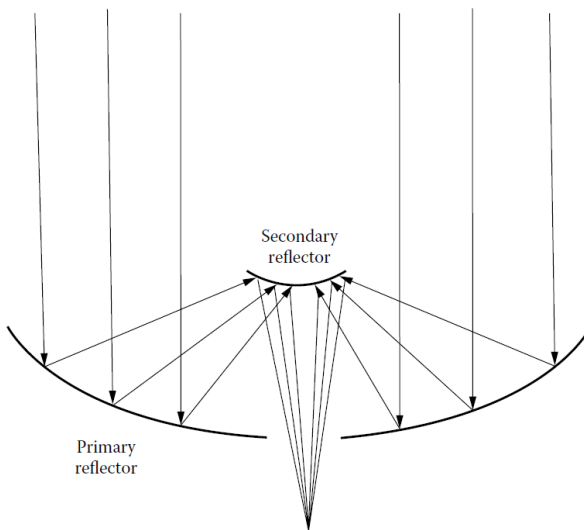


Figure 3.4: Optical Layout of Cassegrain Telescope

The primary reflector serves two important functions. It collects and focuses the radiation from astronomical sources, making it possible to detect faint sources. The amount of radiation collected depends on the telescope's effective area (A_{eff}), which is closely related to the physical area of the primary reflector. As given by Equation 2.2, the power, P , of radiation collected from an astronomical source of flux density F_v is given by

$$P = F_v A_{eff} \Delta v$$

Where:

bandwidth, Δv is the range of frequencies detected.

The bandwidth is determined by the receiver. The larger the physical area of the reflector, the more power is collected from an astronomical source. The effective area of a radio telescope is always smaller than its geometrical area due to various factors involved.

The primary reflector serves a second function, which is to provide directivity, representing a telescope's ability to distinguish emissions from objects at distinct angular positions in the sky. When creating a map using a single radio telescope, the

directivity determines the resolution of the map. Directivity is primarily dependent on the diameter of the telescope and is limited by diffraction. The directivity of a radio telescope is often characterized as the telescope's beam pattern.

3.2 Beam Pattern

The beam pattern is a measure of the sensitivity of the telescope to incoming radio signals as a function of angle on the sky. This is also known as the Point Spread Function. As rays of light from an astronomical source approach the telescope, some rays reflect off the mirror and meet at the focus, while others miss the telescope and hit the ground. The reflector, then, acts like a circular aperture, and the interaction of the light waves meeting at the focus is identical to that when light passes through a circular aperture and meet at a spot on a wall some distance away as a function of angle on the sky. This is true by the reciprocity theorem. The Telescope's Sensitivity Pattern (Figure 3.7) is called the Airy

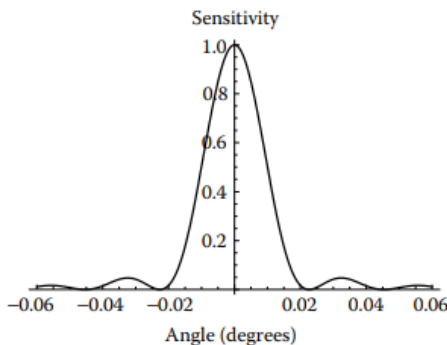


Figure 3.5: Sensitivity Pattern of a Typical Telescope.

Source : Fundamentals of Radio Astronomy - Observational Methods

Disc pattern. The width of the central peak of the Airy pattern is used to define the angular resolution of a single-dish telescope. By convention, the angular width of this peak is taken to be equal to Full Width at Half Maxima(FWHM) of the peak. FWHM is equal to $\frac{1.02\lambda}{D}$, (where D is the aperture) which is smaller than the radius of the Airy Disc, which is $\frac{1.22\lambda}{D}$. In Radio Astronomy, FWHM of the central Airy Peak is used to define the resolution angle of the telescope. This means, that if two sources lie within this angle, the telescopes sees them as one single source in the sky. Since the FWHM of the main lobe is inversely proportional to the diameter of the reflector, we have that large diameter telescopes not only collect more power from an astronomical source, but also provide better angular resolution.. The sensitivity of a Radio Telescope can also be increased by having longer integration times of observation, which can be calculated using Radiometer Equation, which we will come back to later.

3.3 Feeds

At the focus of the telescope, antennas are located to transmit signal from astronomical source to the receiver. These feeds are generally in shape of horns, tapering from a larger end to a smaller end (Figure 3.6). The larger end of

the horn should be atleast of the size of the observing wavelength, which can be quite large in case of radio telescopes. This limits the number of feeds that can be fit into a radio telescope. Diffraction determines the amount of power the feed collects and transmits to the receiver. The beam pattern of the feed determines the illumination pattern of the telescope. The shape of the illumination pattern on the primary reflector affects (1) the angular resolution of the telescope, (2) the sensitivity level in the sidelobes, and (3) the effective collecting area of the telescope.



Figure 3.6: Example of a Circular Feed Horn.

Source : Fundamentals of Radio Astronomy - Observational Methods

Edge Taper is defined as the ratio of the sensitivity at the center of the reflector to that at the edge. A large taper reduces the amount of radiation detected from non astronomical sources such as ground, but also limits the collecting area of the telescope. On the other hand, a small taper whiloe increasing the collecting area of the telescope, also increases the radiation collected from the non astronomical sources, adding to the noise. The optimum edge taper is called 10dB edge taper. For this optimum edge taper, the first sidelobe level is approximately 0.4 percent of the peak, and the maximum collecting area of the telescope is about 82 percent of the reflector's physical area. The FWHM of the central Airy Peak in this case is given by :

$$\theta_{FWHM} = \frac{1.15\lambda}{D}$$

3.4 Surface Errors

The presence of surface errors on the surface of parabolic reduces the on-axis sensitivity of the telescope, and this can be viewed as a loss in the collecting area. The effect of surface errors on the collecting area is described by the Ruze equation, which is given by

$$A_\delta = A_0 e^{-(4\pi\delta z)^2}$$

. The quantity δz is the *rms* of the surface irregularities and measured as deviations from ideal surface of the parabola.

3.5 Noise, Noise Temperature and Antenna Temperature

The electrical power can be described in terms of equivalent temperature by

$$T_{equiv} = \frac{P}{k\Delta v}$$

Where,

k is the Boltzmann Constant and

$\Delta\nu$ is the Bandwidth of the Radiation with Power P .

The equivalent temperature of the power that antenna delivers to the transmission line is described by antenna temperature T_A , while the electrical power due to noise from receiver components is described by the noise temperature T_N . The power due to radiation entering the antenna, which has been amplified by a gain G_1 , is given by: Then, the Power Output P would be

$$P = G_1 k \Delta\nu (T_A + T_N)$$

If we have two amplifiers in succession, the first characterized by G_1 and T_{N1} , and the second by G_2 and T_{N2} , then the noise power due to the first is amplified by a factor of G_2 along with the noise produced by the second amplifier. So the total noise power coming out of the second amplifier is

$$P_N = G_1 G_2 k \Delta\nu T_{N1} + G_2 k \Delta\nu T_{N2}$$

The total gain in succession of devices is therefore just a product of individual gains. Now, if for a succession of devices, we define the *total noise temperature* T_N by

$$P_N = G k \Delta\nu T_N$$

Where, G is the total gain as described above.

Now it remains a trivial calculation to arrive at the formula for *total noise temperature* (just compare the expressions for total noise power) which is given by

$$T_N = T_{N1} + \frac{T_{N2}}{G_1} + \frac{T_{N3}}{G_1 G_2} + \dots$$

With total gain and total noise temperature defined, we can define total detected power as :

$$P = G k \Delta\nu (T_A + T_N)$$

Therefore, even if we observe blank sky, the power out of the receiver is not zero because of the noise power.

The strength of signal from astronomical source relative to the noise level is denoted by σ_P , which is related to bandwidth $\Delta\nu$ of observation and integration time t_i by

$$\sigma_P = \frac{P_N}{\sqrt{\Delta t \Delta\nu}}$$

This is the Radiometer Equation and is essential for planning of any radio observation.

4. Aperture Synthesis (Interferometry)

The technique of *Aperture Synthesis* has had a profound impact on radio astronomy and the studies of the universe. In recognition of its importance, half of the 1974 Nobel Prize in Physics was awarded to Martin Ryle for his development of the method; the other half was awarded to Anthony Hewish for the discovery of pulsars. Some famous Radio Telescopes based on the principle are The Giant Meterwave Radio Telescope (GMRT) located in Pune, The Jansky Very Large Array in San Agustin, New Mexico and the Atacama Large Millimeter/Submillimeter Array (ALMA) located in the Atacama Desert in the Andes of Northern Chile. This technique uses telescopes arranged in an array to produce high resolution images.



Figure 4.1: Jansky Very Large Array in San Agustin, New Mexico.



Figure 4.2: Giant Meterwave Radio Telescope in Pune, India



Figure 4.3: Atacama Large Millimeter / Submillimeter Array (ALMA) located in the Atacama Desert in the Andes of Northern Chile

4.1 Why Aperture Synthesis ?

The main advantage of aperture synthesis is angular resolution. The long wavelengths of Radio Astronomy limit the single-dish observations to very poor resolution. Ground-based observations at visible wavelength can obtain a resolution of 1 arcsec, or 2×10^{-5} radians. For a Radio Telescope to match this resolution, its diameter has to be approximately (using the equation for θ_{FWHM}) :

$$D \approx \frac{10\text{cm}}{2 \times 10^{-5}} \approx 5\text{km}$$

It is practically impossible to build a dish of such a large diameter. Radio astronomers can achieve this high resolution by combining multiple ordinary-sized radio telescopes. By arranging the radio telescopes in an array and treating each pair of telescopes as an interferometer, a new telescope with a significantly larger diameter can be effectively synthesized. This is accomplished by observing the same source with all the telescopes in the array, combining the outputs from each telescope pair, and processing the data mathematically. The outcome of this process is an effective resolution that closely approximates that of a single large telescope whose diameter is equal to the largest distance between antennas in the array. Aperture synthesis produces only the resolution of a large telescope, not the sensitivity. The sensitivity depends on the total collecting area, which, for an array of antennas, is the sum of the effective areas of all the individual antennas.

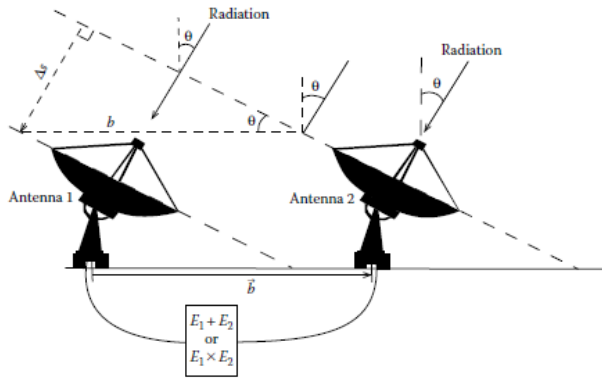


Figure 4.4: Two Element Interferometer receiving signals from a distant radio source at an angle θ relative to zenith

Source : Fundamentals of Radio Astronomy - Observational Methods

4.2 Two Element Interferometer

The basic unit of an aperture synthesis telescope is the two-element interferometer, composed of two antennas separated by a known distance with a known orientation. The vector describing the separation of the antennas is known as the baseline, which is denoted by \vec{b} . Both telescopes are pointed at the same astronomical source in the sky whose direction is defined relative to the midpoint of the baseline connecting the two telescopes. Here we consider the special case in which both the telescopes, the source and the zenith of the midpoint of the baseline lie in the same plane.

A depiction of an interferometric observation in this two-dimensional situation is shown in Figure 4.4. The radio signals approach the telescope along parallel lines due to the astronomical source being essentially at an infinite distance from the telescope. The angle of approach is denoted by θ . The electric fields $E_1(t)$ and $E_2(t)$ are filtered to pass through a defined bandwidth centered at a specific frequency v .

Using the right triangle shown in Figure 4.4, we can express the delay in terms of the direction toward the source. The extra distance Δs is one side of the right triangle in which b is the hypotenuse. So by simple trigonometry, $\Delta s = b \sin \theta$, or

$$\tau = \frac{b \sin \theta}{c}$$

This time delay in the arrival of the wave front means there will be a phase difference, $\Delta\Phi$, between the two signals, given by

$$\Delta\Phi = \frac{2\pi \Delta s}{\lambda}$$

If Δs equals one wavelength, then the wave front entering antenna 2 will be 2π radians ahead of the same wave front entering antenna 1. We can also express the phase difference in terms of the time delay by

$$\Delta\Phi = 2\pi v \tau$$

If we choose the time when the wave enters antenna 1 as defining zero phase, then we must add the phase shift to the wave entering antenna 2. Therefore, we have that the electric fields arriving at the combination point are given by

$$E_1 = E_0 \cos(2\pi v t)$$

$$E_2 = E_0 \cos(2\pi v(t + \tau))$$

The angle θ changes with rotation of Earth, therefore the phase difference between signals from two antennas also changes with time. To calculate the net response we add or multiply these two signals and then take average.

4.2.1 Response of Multiplicative Interferometer

Multiplying the Electric Fields entering the two antennas, we get

$$E_1 \cdot E_2 = E_0^2 \cos(2\pi v t) \cos[2\pi v(t + \tau)]$$

Using Basic Trigonometry, we can write this as

$$E_1 \cdot E_2 = \frac{E_0^2}{2} \cos(4\pi v t + 2\pi v \tau) + \frac{E_0^2}{2} \cos(2\pi v \tau)$$

The product of the electric fields is averaged over a period of time, called the integration time (the time of observation). The first term averages to zero, and so only the second term remains.

It's very important to note here that the added signals are averaged over time t , while τ , the delay for the wave front to reach antenna 1, is relatively constant over the integration time (although it changes slowly as the Earth rotates). The term $\cos(2\pi v \tau)$, therefore, does not go to zero when time averaged.

Therefore, the detected power of multiplicative interferometer is :

$$\langle E_1 \cdot E_2 \rangle = \frac{E_0^2}{2} \cos(2\pi v \tau)$$

The delay is related to the extra path length by $\tau = \frac{\Delta s}{c}$, where $\Delta s = b \sin \theta$, allowing us to write

$$\langle E_1 \cdot E_2 \rangle = \frac{E_0^2}{2} \cos\left(2\pi \frac{b}{\lambda} \sin \theta\right)$$

4.3 Fringe Pattern

The pattern displayed in Figure 4.5 is reminiscent of the double-slit interference pattern; waves from the same source are passed through two apertures and recombined and yields an oscillating pattern that depends on angle. These oscillations are called fringes, and the time-dependent function

$$\cos\left[2\pi \frac{b}{\lambda} \sin(\omega_E t)\right]$$

is called the fringe function.

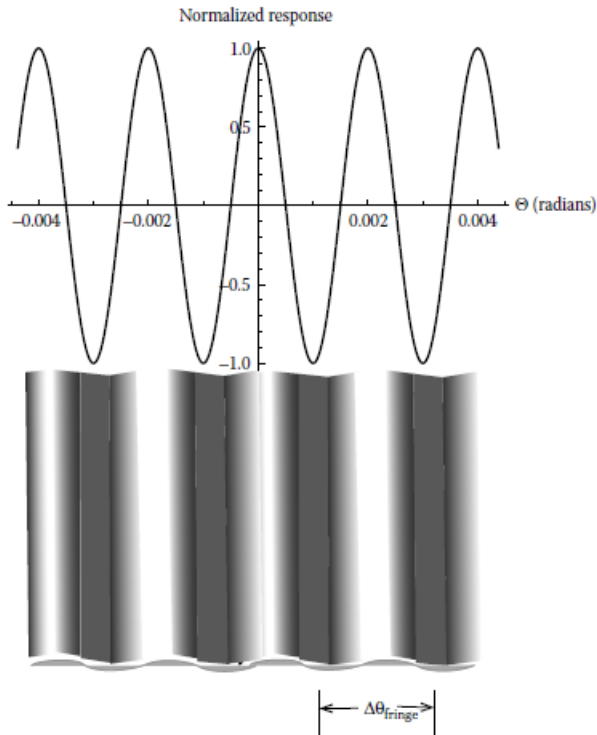


Figure 4.5: Oscillating pattern of the interferometer response as a function of the position of the point source. This is known as the fringe pattern. The fringe spacing, $\Delta\theta_{fringe}$, is indicated.

Source : Fundamentals of Radio Astronomy : Observational Methods

4.3.1 Calibration

By observing a point source with a known flux density and fitting the fringe oscillations to the expected time dependence, we can calibrate a multiplicative interferometer. This calibration yields a conversion factor R that relates the fringe amplitudes to the flux density.

$$R = F_v \cos[2\pi \frac{b}{\lambda} \sin(\omega_E t)]$$

4.4 Visibility

We define a new term, Visibility $V(u, v)$ which is a complex term and is related to the fringe amplitude and average intensity at a given point u, v on the uv plane.

$$V(uv) = \sum_{ij} V_{ij}(u, v, t, \delta t, v, \delta v) = \langle V_i(., t, .) V_j^*(., t + \tau, .) \rangle$$

Note that the expression for V_{ij} is exactly the same as the result which we calculated in Section 4.2.1, just represented as a complex number to represent both Amplitude and Phase. $V(u, v)$ is just $V_{ij}(u, v)$ summed over all pairs of telescopes. The Equation

$$V_{\frac{b}{\lambda}} = F_v \cos(2\pi \frac{b\Delta\theta}{\lambda})$$

is called the Visibility Equation.

The Visibility $V(u,v)$ is directly related to the brightness of the source. In particular for small fields of view, it turns out that that the visibility $V(u,v)$ is the 2D Fourier Transformation of the brightness of the sky $T(x,y)$. Thus if we are able to find $V(u,v)$, we can just make an Inverse Fourier Transformation and obtain $T(x,y)$, which is the brightness of the source in the image plane, or in simple words the image of the source!

$$T(x,y) \longleftrightarrow V(u,v)$$

$$V(u,v) = \int \int T(x,y) e^{2\pi i(ux+vy)} dx dy$$

$$T(x,y) = \int \int V(u,v) e^{-2\pi i(ux+vy)} du dv$$

4.5 Synthesising Image

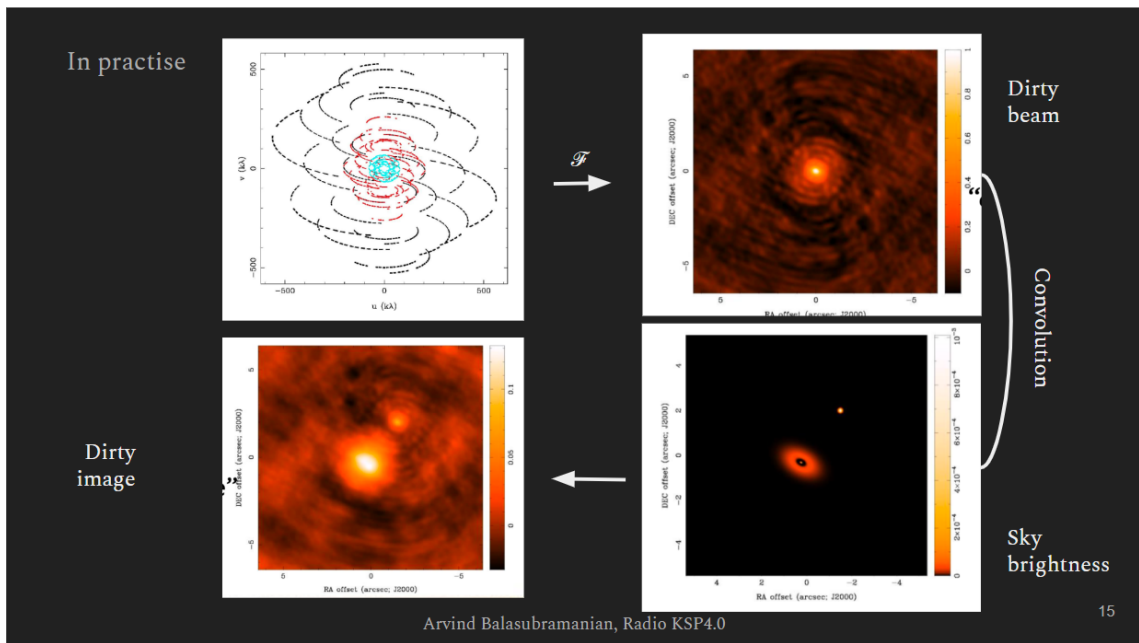


Figure 4.6: Process of Image Synthesis involving Fourier Transform from U-V Plane to get the Dirty Image, and deconvolution of Dirty Image to get Actual Sky Brightness

Due to the limited observation time, we cannot completely fill the U-V Plane, therefore we cannot calculate the exact sky brightness, the resultant $T'(x,y)$ we get is the 'Dirty Image'. It can be seen that the 'Dirty Image' is just a convolution of the Point Spread Function (Dirty Beam) and the Actual Sky Brightness. Therefore, the cleaning process of an image is deconvolution of dirty beam from the dirty image.

4.5.1 Casa Activity

We performed the Cleaning process on an image in CASA. Below we show the ‘DirtyImage’ and the image we get after deconvolution process.

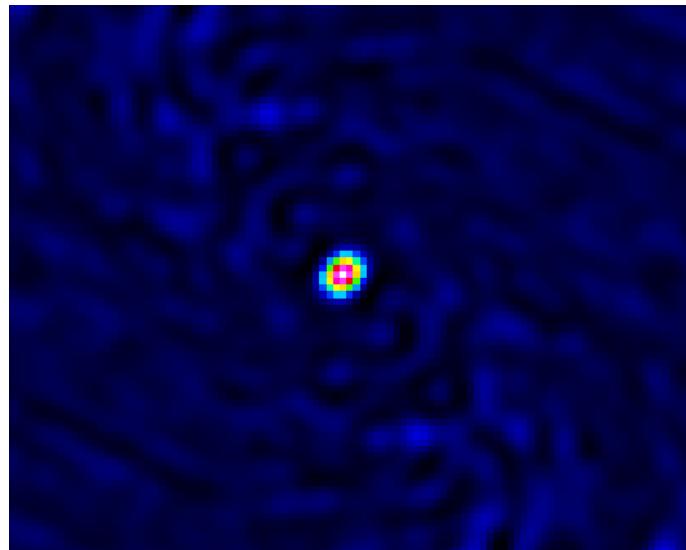


Figure 4.7: Dirty Image

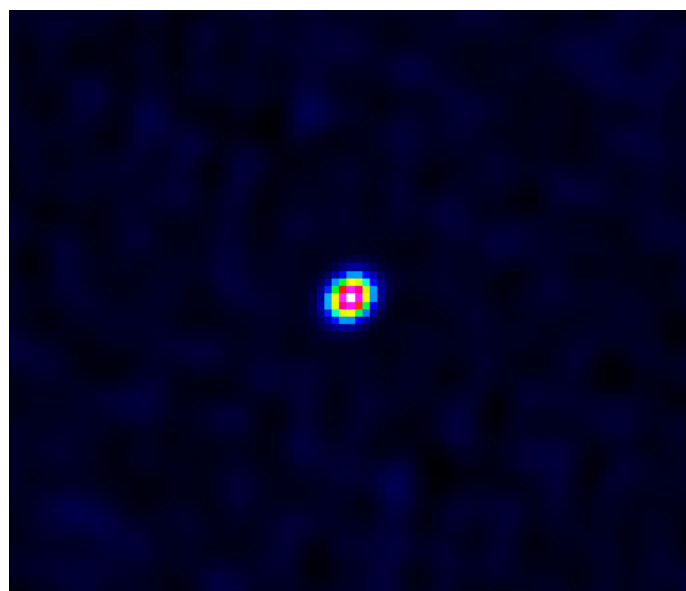
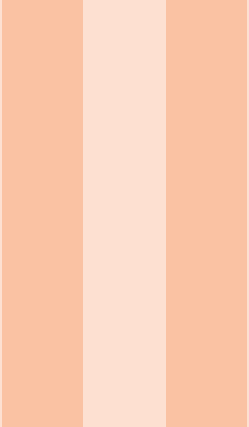


Figure 4.8: Cleaned Image after Deconvolution Process



Part Two

5	GW170817 - Binary Neutron Star Merger	37
5.1	Introduction	
5.2	What are Light Curves ?	
5.3	Markov Chain Monte Carlo	
5.4	Smooth Broken Power Law	
5.5	Data Analysis	
6	Fast Radio Bursts	43
6.1	What are Transients ?	
6.2	Dispersion Measure	
6.3	Activity - Finding DM of a Burst	
	Bibliography	47
	Books	



5. GW170817 - Binary Neutron Star Merger

5.1 Introduction

GW 170817 was a gravitational wave (GW) signal observed by the LIGO and Virgo detectors on 17 August 2017, originating from the shell elliptical galaxy NGC 4993. The signal was produced by the last minutes of a binary pair of neutron stars' inspiral process, ending with a merger. It is the first GW observation that has been confirmed by non-gravitational means. Unlike the five previous GW detections, which were of merging black holes not expected to produce a detectable electromagnetic signal.

5.2 What are Light Curves ?

Light Curves are graphs that show brightness of an astronomical source over a period of time. The record of changes in brightness that a light curve provides can help astronomers understand processes at work within the object they are studying and identify specific categories (or classes) of stellar events. We know generally what light curves look like for a set of objects, so when we plot a new light curve, we can compare it to those standard light curves to possibly identify the type of object we're observing.

We already plotted the light curve for GW170817 before. We plotted data points from Chandra and Janksy VLA in X-Ray and Radio Respectively. The scatter plot of the data points is as shown below.



Figure 5.1: Light Curve of GW170817

5.3 Markov Chain Monte Carlo

Markov Chain Monte Carlo (MCMC for short) is a method for fitting models to data. MCMC is different from a simple linear least squared fit. MCMC is a parameter space exploration tool - a sampler.

The procedure of conducting an MCMC involves evaluating generated models against the available data. These models are created using a specific set of parameters, and typically, our objective is to identify the set of parameters that yield the model that best matches our data.

It's important to emphasize that for the MCMC process to be workable, it follows a Bayesian approach rather than a frequentist one. This entails incorporating what are known as priors on our parameters. These priors encode the information that we believe we already possess about the system we are attempting to model.

We then calculate the probability of our model given our data. The process is something like this:

- Establish a function that produces a model based on a given set of input parameters.
- Create an ensemble of walkers represented by a vector θ , containing a set of parameters utilized by the model-generating function. These walkers explore the parameter space, and we can envision a "grid" of possible values for θ , within the range specified by the priors.
- Each walker initiates the exploration of the parameter space by taking a "step" to a new value of θ and generates a model using that parameter set.

The model's resemblance to the given data is assessed, via a simple χ^2 -type check

$$\text{"Likeness"} = -\frac{1}{2} \left(\frac{y_{\text{data}} - y_{\text{model}}}{y_{\text{data,err}}} \right)^2$$

- The MCMC algorithm then compares the likeness of the new model with the data to that of the previous model. If the new location demonstrates a better match, the walker moves to that position and repeats the process. Conversely, if the new location results in a worse fit, the walker reverts to its previous position and attempts a different direction.
- Gradually, all walkers tend to converge towards the regions of highest "likeness" between the models generated and the observed data.

Upon concluding the process (known as a production run), we obtain a posterior distribution or chain. Each walker retains a record of every θ vector it explored and the corresponding likelihood of the model given the observed data at that specific θ value.

Assuming the MCMC runs long enough to converge reasonably, the distribution represents a sample of reasonable models to describe our data. It is reasonable to wonder what the "best fit" is. But we need to remember that MCMC is not a "fitter," it is a "sampler." MCMC can't tell us that parameter set θ is the "best" - one our models will have the numerically highest value of "likeness" to the data, but if we ran the MCMC, or ran it longer duration, we will get different answers. What MCMC is better at telling us is something like "If you draw 100 random models out of the posterior distribution, the spread in those models is representative of our ability to constrain the parameters in those models."

5.4 Smooth Broken Power Law

We will be fitting the GW170817 Light Curve with a model called *Smooth Broken Power Law* model, which is parameterised as follows :

$$F(t, v) = 2^{\frac{1}{s}} \left(\frac{v}{3\text{GHz}} \right)^\beta F_p \left[\left(\frac{t}{t_p} \right)^{-s\alpha_1} + \left(\frac{t}{t_p} \right)^{-s\alpha_2} \right]^{-\frac{1}{s}}$$

where v is the observing frequency, β is the spectral index, F_p is the flux density at 3 GHz at light curve peak, t is the time post merger, t_p is the light curve peak time, s is the smoothness parameter, and α_1 and α_2 are the power-law rise and decay slopes, respectively.

5.5 Data Analysis

Shown below, we have the scatter plot of log-log Light Curve of GW170817 with data of Flux Density measured from the Jansky VLA, indicated by the blue points. The Best Fit found by Scipy Curvefit is shown in Red. The parameter values obtained from Scipy Curvefitting can be used as prior values for MCMC.

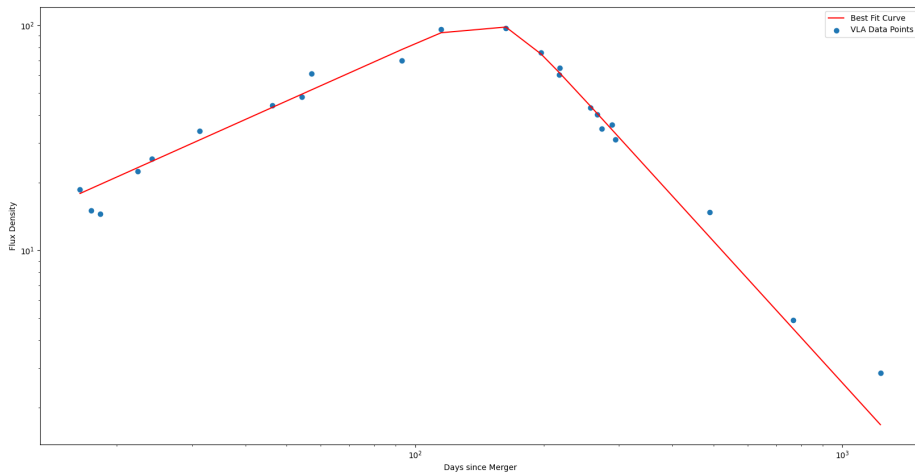


Figure 5.2: Log-Log Plot of GW170817 Light Curve

Now we are ready to apply MCMC to our data. We have used documentation of library emcee to code for MCMC. MCMC outputs sets of values of parameters which likely fit our data (if MCMC converges sufficiently). Shown below, we have plotted a hundred samples output by MCMC, and we can see that it does a good job of matching our data. We can also see that the graphs seem to overlap each other.

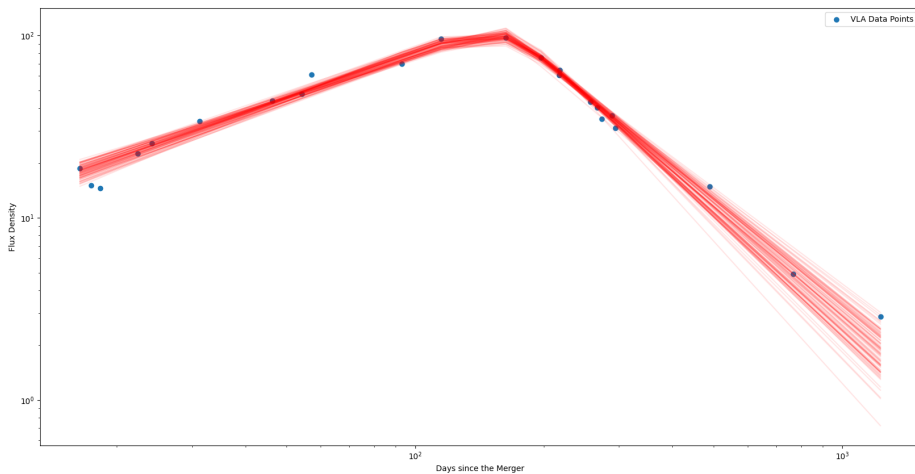


Figure 5.3: Models output by MCMC after exploring the parameter space

Now we can find the "most likely" set of parameters for our data, i.e. the sample from the posterior distribution chain having the highest probability of fitting the data. In figure 5.4 we have shown plotted the most-likely output given by MCMC (which can be different every time you run MCMC) and the Best Fit Curve we got earlier. The fact that overlap each other well is sufficient to show that the MCMC chains have converged satisfactorily.

Corner Plots

We used corner.py module to visualize 1D and 2D spreads between the parameters. The plots we got are shown below.

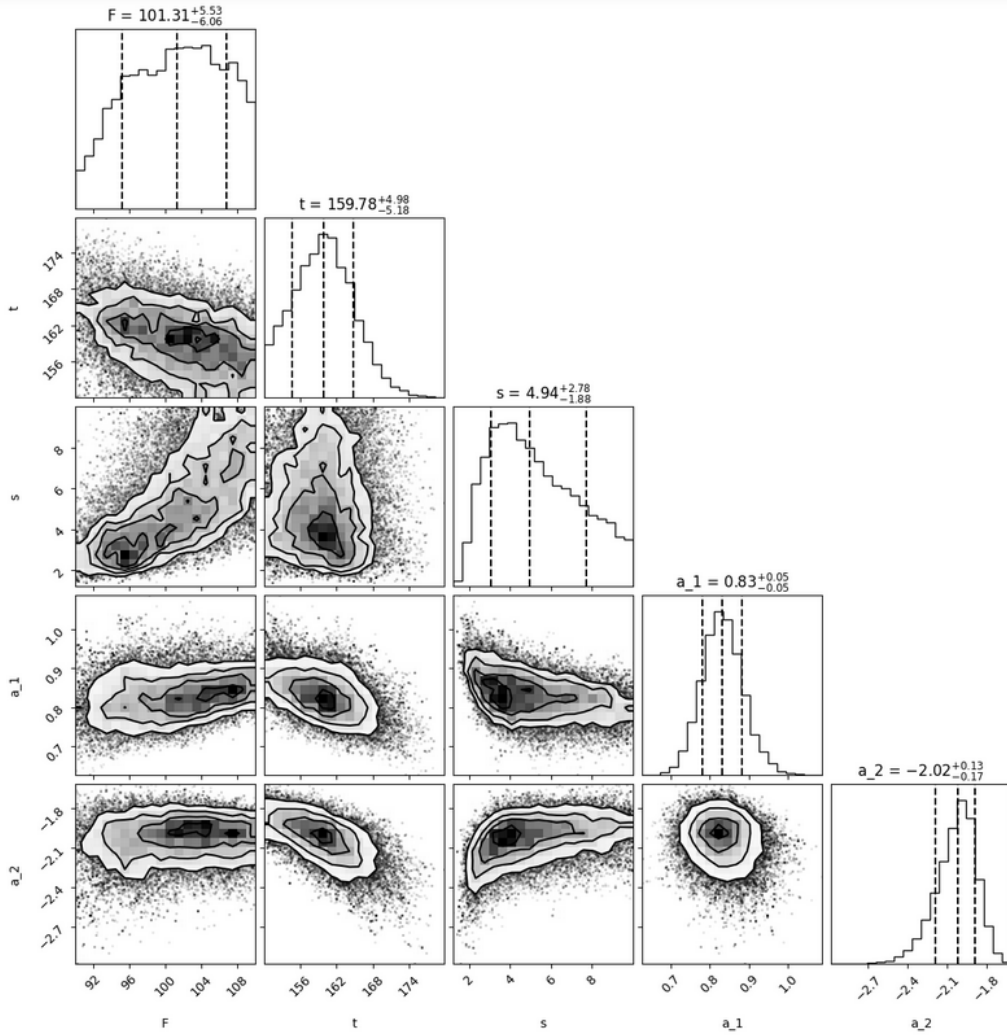


Figure 5.4: Plots of 1D and 2D Spread between parameters using corner.py module

These plots are helpful in finding dependencies between various parameters used in our model and to get some uncertainties in our parameter estimation. For example, we can see that the corner plots hint towards an inverse relationship between α_1 and t (peak), and a direct correlation between Flux Density at 3GHz light curve peak (F_p) and smoothness parameter s .



6. Fast Radio Bursts

6.1 What are Transients ?

Transients are key frontier of modern research in Astronomy and Astrophysics with far-reaching implications for our understanding of the life and death of stars, the birth of neutron stars and black holes, the production of the chemical elements, the expansion history of the universe, the properties of the first stars and galaxies, and the epoch of cosmic re-ionization. Transients refer to astronomical phenomena with durations of fractions of a second to weeks or years. Typically they are extreme, short-lived events associated with the total or partial destruction of an astrophysical object. The events can generate emission at all or specific wavelengths both in electromagnetic radiation and gravitational waves. They can appear to be extremely bright and can be observed over cosmological distances. They are key objects of interest in Multi-Messenger Astronomy. Some examples of Transients include Gamma ray Bursts, Merger of Binary Neutron stars, supernovae and Fast Radio Bursts.

Pulsars are rapidly rotating neutron stars that emit beams of radio radiation from their magnetic poles, at low frequencies. Transients in radio bands are mainly dominated by three kinds of emission mechanisms. Slow transients majorly emit via incoherent synchrotron mechanism and are limited by the brightness temperature. These events are mainly associated with explosive events, such as Gamma Ray Bursts, supernovae, X-ray binaries, tidal disruption events etc. In addition, novae and symbiotic stars show slow variability and are dominated by thermal emission. Fast transients are usually associated with coherent emission and show relatively fast variability, high brightness temperature and often show high polarization associated with them, such as Fast Radio bursts, flare stars etc.

6.2 Dispersion Measure

Transients can generate electromagnetic radiation across the entire electromagnetic spectrum and can generate signals in other messengers like Gravitational Waves as well. The surprising fact here is that the arrival time of signal of different frequencies of electromagnetic waves is not the same and is dependent on the frequency of the electromagnetic wave.

Dispersion Measure (DM) is defined as :

$$DM = \int n_e dl$$

where n_e is the electron density.

The Time of Arrival (t_{arr}) is directly proportional to Dispersion Measure (DM) and inversely proportional to the square of frequency(ν) of the electromagnetic wave.

$$t_{arr} \propto DM\nu^{-2}$$

We can see that, according to the relation, high frequency waves come before the low frequency waves. DM can be used as a proxy for distance. Lower the DM, lower is the distance between us and the Transient Source. The DM signifies how much matter the light from the FRB or pulsar interacted with on its way to our telescope.

The constant of proportionality is 4.148808×10^3 , if your arrival time is in seconds, frequency (ν) is in MHz and DM is pc cm $^{-3}$ (pc is parsecs).

In the Figure 6.1 , DM Values corresponding to various Transients are shown.

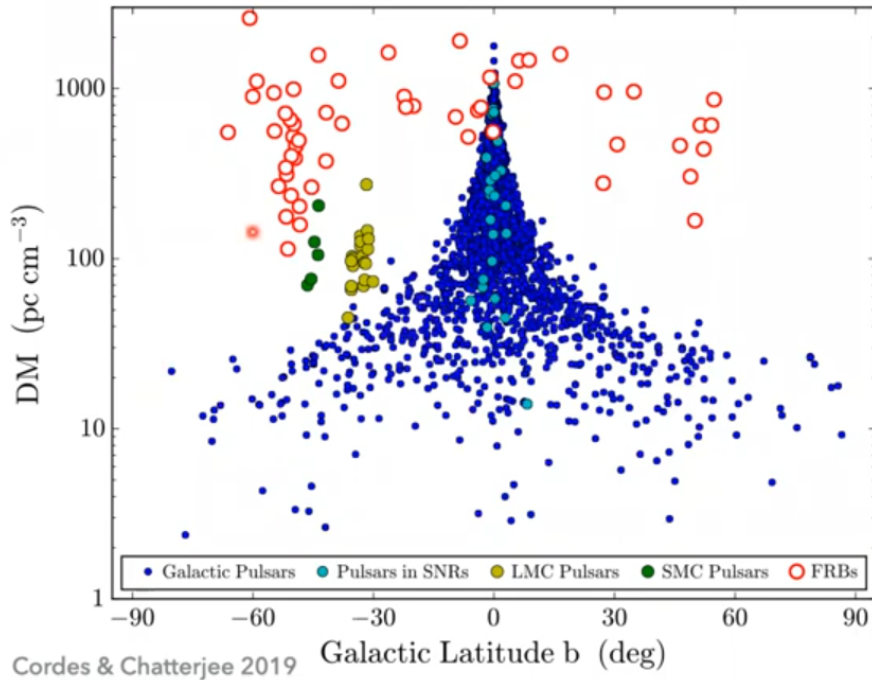


Figure 6.1: Plot of DM Values of various Astronomical Phenomenon
Credits : Cordes and Chatterjee 2019

6.3 Activity - Finding DM of a Burst

We will be using some data of a pulsar B0011+47

Shown in Figure 6.3 is the Waterfall Plot of the data collected on B0011+47. Y- axis has the 32 bins of frequency from 800 to 400 MHz , while X-axis represents time in milliseconds with each bin being 16ms long. As discussed before we can see, we receive electromagnetic waves with higher frequency first.

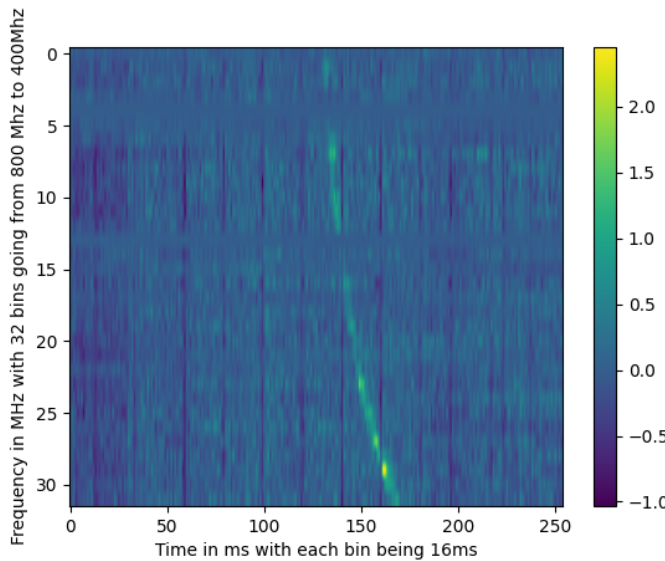


Figure 6.2: Waterfall Plot of Data of B0011+47 from CHIME

In the next step, we calculated the delay corresponding to each frequency relative to the highest frequency in the dataset, which in our case is 800Hz. To do so, we use the equation relating t_{arr} , DM and v shown before. After calculating the delays corresponding to each frequency, we shift the frequency channels by the calculated delays. At the correct DM Value, the pulses will line up. We have shown this in Figure 6.4, where the pulses lined up for DM value of approximately 30 pc cm^{-3} .

We can now calculate the Time-series. Time series can be calculated by summing over all frequency channels. We can define a signal-to-noise ratio (SNR) for this time series by taking the ratio of the maximum of the absolute value of the time series to the mean of the absolute value of the time series. We repeat this SNR calculation for many DMs and find the DM where SNR is maximum. This de-disperses the data and the best DM will give a nice peak in the time series.

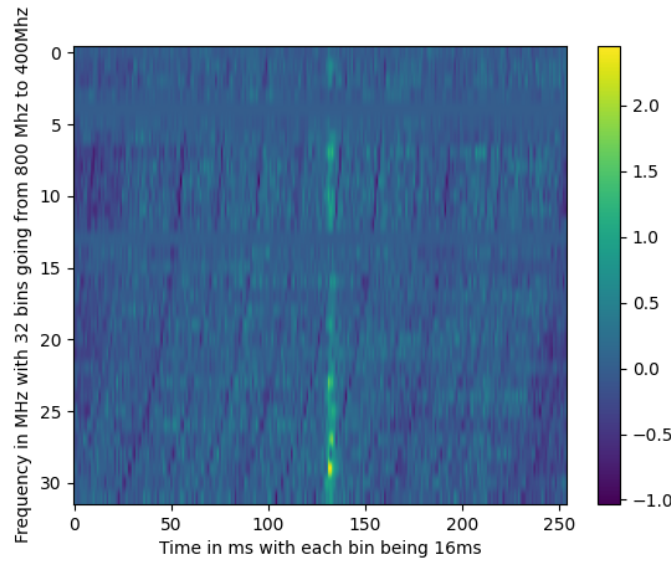


Figure 6.3: Lining Up of Pulses at Correct DM Value

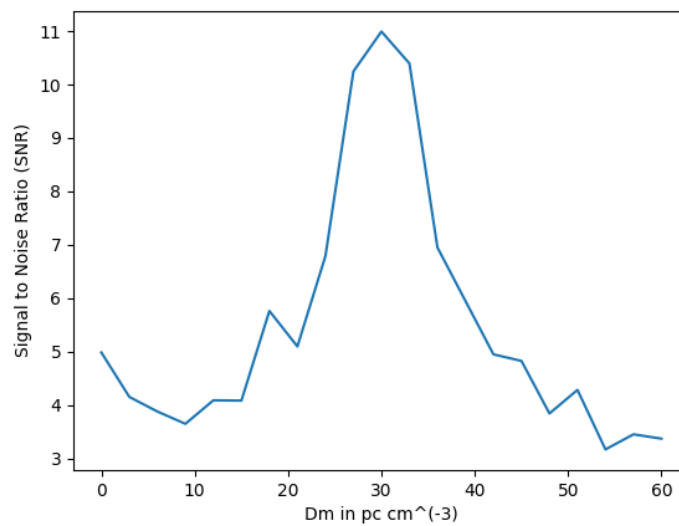


Figure 6.4: Plot of SNR v/s DM Values



Bibliography

Books

Marr, Jonathan M., Snell, Ronald L., Kurtz, Stanley E.. Fundamentals of Radio Astronomy: Observational Methods. United Kingdom: CRC Press, 2015.